# A Newton–Galerkin Method for Fluid Flow Exhibiting Uncertain Periodic Dynamics[*]

M. Schick[†], V. Heuveline[‡], and O. P. Le Maître[§]

**Abstract.** The determination of limit-cycles plays an important role in characterizing complex dynamical systems, such as unsteady fluid flows. In practice, dynamical systems are described by models equations involving parameters which are seldom exactly known, leading to parameteric uncertainties. These parameters can be suitably modeled as random variables so, if the system possesses almost surely a stable time periodic solution, limit cycles become stochastic too. This paper introduces a novel numerical method for the computation of stable stochastic limit-cycles based on the spectral stochastic finite element method with polynomial chaos (PC) expansions. The method is designed to overcome the limitation of PC expansions related to convergence breakdown for long term integration. First, a stochastic time scaling of the model equations is determined to control the *phase-drift* of the stochastic trajectories and allowing for accurate low order PC expansions. Second, using the rescaled governing equations we aim at determining a stochastic initial condition and period such that the stochastic trajectories close after completion of one cycle. The proposed method is implemented and demonstrated on a complex flow problem, modeled by the incompressible Navier-Stokes equations, consisting in the periodic vortex shedding behind a circular cylinder with stochastic inflow conditions. Numerical results are verified by comparison to deterministic reference simulations and demonstrate high accuracy in capturing the stochastic variability of the limit-cycle with respect to the inflow parameters.

**1. Introduction.** The numerical simulation of physical systems requires a mathematical model and the provision of all information and values for the parameters involved in the model definition. Fluid flow simulations, for instance, usually require to prescribe domain geometry, boundary and initial conditions, external forcing and source terms, constants in constitutive equations and physical models, ... In many cases, these model inputs are not completely known and can only be expressed with some uncertainty arising from either a lack of knowledge

(epistemic uncertainty) or intrinsic variability (aleatoric uncertainty). Epistemic uncertainties, resulting *e.g.* from model simplifications, measurement errors and calibration procedures, can be reduced by improving the physical modeling or/and providing more information on the actual properties of the system investigated. In contrast, uncertainties of aleatoric type have a random nature, are not reducible, and the system is not deterministically predictable. In any cases, quantifying the impact of these uncertainties on the model predictions is an important task for the exploitation, fair analysis and subsequent decision making. This fact has motivated the development of Uncertainty Quantification (UQ) methods for numerical simulations, in particular probabilistic approaches where the uncertain model inputs are given probability laws which are propagated through the model to characterize the output uncertainty.

In this paper we rely on stochastic spectral expansions and so called Polynomial Chaos (PC) expansions [33] to represent the uncertainty in the model output due to random input parameters. PC expansions express the dependence of the model solution (or of some quantity of interest) with respect to the uncertain parameters as series involving predefined polynomials in the random parameters. Following the seminal work of Ghanem and Spanos [9], standardized independent parameters and orthogonal multivariate polynomials are classically considered. PC expansions can exhibit high (spectral) converge rate when the output is sufficiently smooth with respect to the random parameters, making the PC approach possibly more efficient than its alternatives (*e.g.* Monte-Carlo methods). Determination of the PC expansions, however, increases the computational complexity compared to solving the original deterministic problems, and requires efficient algorithms. Classically, computational methods for PC are separated into two classes: the non-intrusive methods and the Galerkin methods (see references in [15]). Non-intrusive methods rely of a sample set of deterministic simulations to construct the PC expansion (*e.g.* by regression, discrete projection, interpolation, ...), while Galerkin methods are based on a reformulation of the stochastic problem. In the present paper, we consider Galerkin projections at the stochastic level for the resolution of fluid flows having random parameters. For the Galerkin method, the stochastic governing equations are projected on the space spanned by the PC basis, resulting in a fully coupled system of deterministic governing equations for the PC coefficients of the solution. The computational cost is then related to the dimension of the PC basis, or number of modes in the PC expansion, which is function of the number of random parameters and of the polynomial degree of the PC expansion. In fact, the size of the coupled system is the principal limitation for the application of the Galerkin approach to complex problems.

In Computational Fluid Dynamics, stochastic Galerkin approaches were demonstrated for the resolution of the viscous incompressible [16] or weakly compressible Navier-Stokes equations [21] (see also references in the review articles [14, 22]). Non-smooth flows (hyperbolic models) were more recently considered and require specific treatments (*e.g.* stochastic multi-resolution scheme) to handle discontinuities and non-smooth dependences on the random parameters. We shall restrict here to smooth flows governed by the incompressible Navier-Stokes equations. The dynamic of these flows highly depends of the Reynolds number, which is defined as a ratio of characteristic inertial and viscous stresses. At low Reynolds numbers the flows have steady state solutions, which destabilize and become time-dependent as the Reynolds number increases. Increasing further the Reynolds number, flows become chaotic with a transition to turbulence. Beside the increasing flow complexity, the sensitivity of

the flow to initial, boundary conditions and external forcing generally increases too with the Reynolds number. This effect prevents direct PC approximation of the Navier-Stokes solution for high Reynolds number flows (though the PC projection of integral and statistical quantities is still possible, provided they depend smoothly on the uncertain parameters). The issue is related to the fact that trajectories of the flow corresponding to close but different realizations of the uncertain model inputs can continuously (exponentially in the chaotic regime) separate in time, requiring a prohibitively large polynomial degree for the PC expansion to accurately capture the evolutions in time of the inputs dependencies.

Among complex dynamics, stable limit-cycles play an important role in the study of flow transition from laminar to turbulent regimes and limit-cycle oscillations in flow-induced vibration analyses. These dynamics occur at moderate Reynolds numbers and are characterized by time-periodic solutions with a fixed frequency (or period). Because of their importance in dynamical studies, several numerical methods have been proposed to compute deterministic limit-cycles, see for example [3, 4]. This work focuses on the computation of such limit cycles in the presence of uncertain random inputs. Because of the uncertainties, the limit-cycles generally become random quantities; we shall assume that the dynamic is almost surely time-periodic, *i.e.* there exists a time-periodic solution for every realization of the random inputs except for some set of event with probability equal to zero. In this situation, stable stochastic limit-cycles can be determined in principle by means of time-integration of the governing equations: almost all trajectories should converge asymptotically to the limit-cycle. However, it is known that this straightforward approach may not be practical in the context of PC expansions because of the so-called long term integration issue [18]: if the uncertain parameters yield a limit-cycle with uncertain period, a growing PC order is required as time advances. This is due to the phase-drift between distinct trajectories of the flow for different realizations of the input parameters. Several approaches have been proposed to tackle the effect of the phase-drift. In [32] a multi-element approach was introduced, which is able to postpone the point of convergence breakdown to later simulation times by using a domain decomposition of the probability space and local approximations. In [2], a similar idea was developed employing a wavelet multi-resolution analysis [17, 19], which, however, also suffers from the same drawback regarding the long term integration issue. More recently, time-dependent bases for capturing the time evolutions of the probability distribution of the solution was introduced in [8, 27]. In [11] an extension of the method in [8] was proposed, which combines time-dependent basis functionals with the domain decomposition introduced in [32] to improve numerical stability.

All these treatments of the long term integration issue allow one to compute stable limit-cycles by means of classical time integration, owing to a sufficient enrichment of the stochastic basis or a possibly costly time adaption of the basis functionals. In fact, none of these treatments addresses the central difficulty which is related to the *phase-drift* between realizations. Our claim is that, in many situations, random phase information has no relevance and can be set arbitrarily, while only the dependencies of the limit-cycle on the uncertain parameters are of interest. In such cases, the random limit-cycle can be simply defined by determining an arbitrary random initial condition, belonging to the limit-cycle, and the random period. The potential advantage for this description of the dynamics lies in the fact that the random solution at any phase can be subsequently recovered by time integration from the initial condition over *at most* one period, thus avoiding the need of particular treatment required

for long term integration. The principal focus of the present work is then to demonstrate the validity of this description and to verify that it allows to compute uncertain limit-cycles with low degree PC expansions. To the present knowledge of the authors, there do not exist dedicated numerical algorithms for computing the PC expansion of a stochastic limit-cycle with uncertain period. Defining the period and initial condition on the limit-cycle as the solution of a constrained optimization problem, we introduce a numerical algorithm for the determination of these two quantities. The solution of the optimization problem is discretized using the spectral stochastic finite element method (SSFEM), with Galerkin projections of the governing equations on the PC basis. The main ingredients of the proposed algorithm are then a stochastic rescaling in time of the unsteady incompressible Navier–Stokes equations (using the unknown stochastic period), a Newton solver, and an appropriate enforcement of the optimality constraint. In addition, inspired by the ideas proposed in [18] we introduce a secondary stochastic time scaling to control the *phase-drift* in an $L^2$-sense with respect to some deterministic reference trajectory. This secondary time scaling improves the first re-scaling by the stochastic period and enable computations up to machine precision. The convergence properties of the algorithm are verified for a two-dimensional spatial flows around a circular domain with stochastic inflow boundary conditions yielding a laminar, time-periodic vortex shedding, known as a Kàrmàn vortex street.

The paper is structured as follows. Section 2 introduces the unsteady stochastic incompressible Navier–Stokes equations along with the problem definition of finding almost time-periodic solutions (limit-cycles). Section 3 describes the numerical method for computing the PC expansion of an initial condition and the period of the random limit-cycle, together with the control of the *phase-drift*. The convergence properties of the algorithm are verified using adequate benchmark problems in section 4. Finally, section 5 provides a short summary and conclusions of this work.

## 2. Model equations and problem definition.

### 2.1. Unsteady stochastic incompressible Navier–Stokes equations.
It is assumed that there exists a stochastic model, which appropriately describes the underlying uncertainties within the considered system. Furthermore, it is assumed that the uncertainties can be parametrized via some random vector $\xi = (\xi_1, \ldots, \xi_L) \in \mathbb{R}^L$ of dimension $L \in \mathbb{N}$, where $\xi_i$, $i = 1, \ldots, L$, are independent real-valued random variables and $\xi$ belongs to some underlying probability space $(\Omega, \mathcal{F}, \mathbb{P})$, *i.e.* the probability distribution for $\xi$ is given. The uncertainties shall be introduced via boundary or initial conditions. The parametrized unsteady stochastic incompressible Navier–Stokes equations (SNSE) read as

$$\begin{aligned}
(2.1) \quad & \partial_t u(x,t,\xi) + (u(x,t,\xi) \cdot \nabla)u(x,t,\xi) - \nu \Delta u(x,t,\xi) + \nabla p(x,t,\xi) = 0 && \text{in } \mathcal{D}, \\
(2.2) \quad & \nabla \cdot u(x,t,\xi) = 0 && \text{in } \mathcal{D}, \\
(2.3) \quad & u(x,t,\xi) = g(x,t,\xi) && \text{on } \Gamma, \\
(2.4) \quad & u(x,t=0;\xi) = u_I(x,\xi) && \text{in } \mathcal{D}
\end{aligned}$$

for $t > 0$ almost surely in $\Omega$. Here, $\mathcal{D} \subset \mathbb{R}^d$, $d = 2, 3$, denotes the spatial domain with Dirichlet boundary $\Gamma \subset \partial \mathcal{D}$.

Note that the velocity vector $u = u(x, t; \xi)$ and the pressure $p(x, t; \xi)$ are random fields due to their implicit dependences on the random vector $\xi$ through the partial differential equation. The SNSE can be solved relying on PC expansions of the velocity and pressure fields and using the stochastic Galerkin projection method (see, e.g., [14, 16, 20] and references in [15]). However, as discussed in the introduction, if the SNSE possess no stable steady solution a high order PC expansion is expected to be necessary for long term integration, even if the individual realizations exhibit almost surely asymptotically periodic dynamics. This fact motivates the direct determination of the stochastic periodic solutions instead of proceeding from straightforward time integration of the PC system.

**2.2. Periodic solutions.** We introduce a new numerical method for determining solutions of the SNSE, which are almost surely periodic, by extending a deterministic approach introduced by Duguet, Pringle, and Kerswell [4] to the framework of the SSFEM [9]. This makes possible a functional representation of the stochastic period and initial condition with respect to the random input by using a PC expansion.

For convenience, we use abbreviated notations of repeatedly occurring vector spaces:

$$\mathcal{S} := L^2(\Omega), \quad V := H^1(\mathcal{D}), \quad V_0 := H_0^1(\mathcal{D}), \quad W := L^2(\mathcal{D}).$$

A fundamental assumption about existence of a time-periodic solution needs to hold.

*Assumption* 1. There exist a solution $u$ to (2.1)–(2.4), $u(\cdot, t, \cdot) \in V \otimes \mathcal{S}$, $t \geq 0$, and a bounded period $T \in \mathcal{S}$ with $\alpha \leq T < \infty$ almost surely for some $\alpha > 0$ such that for $t \geq 0$,

$$u(x, t + T(\xi); \xi) = u(x, t; \xi) \quad \forall x \in \overline{\mathcal{D}} \quad \text{almost surely.}$$

The main problem in computing stochastic periodic orbits arises from the stochastic nature of the period $T$. A discretization based on a deterministic time stepping method will have difficulties in capturing the stochastic variations of the period, since the trajectories of a solution to the SNSE depend on a random event $\omega \in \Omega$. The approach outlined in the following aims at representing the stochastic period as some additional random input within the SNSE, introducing a new random variable, whose computation introduces an additional condition. This allows the use of a deterministic simulation time interval to compute an initial condition and a period, since the uncertainty within the time interval is transferred towards the system equations.

We introduce a new scaled time variable $\lambda$ which is defined for $t \geq 0$ by

$$(2.5) \qquad \lambda(t, \xi) := \frac{t}{T(\xi)}, \quad \text{point-wise in } \Omega.$$

Note that $\lambda$ is a random process and $\lambda(t, \cdot) \in \mathcal{S}$ for $t \geq 0$, provided that the period $T$ satisfies Assumption 1. Introducing the scaled time $\lambda$ into (2.1)–(2.3) results in a scaled version of the unsteady stochastic incompressible Navier–Stokes equations (S-SNSE) for $\lambda > 0$:

$$\partial_\lambda \tilde{u}(x, \lambda, \xi) + T(\xi)(\tilde{u}(x, \lambda, \xi) \cdot \nabla)\tilde{u}(x, \lambda, \xi)$$

$$(2.6) \qquad\qquad - \nu T(\xi)\Delta \tilde{u}(x, \lambda, \xi) + \nabla \tilde{p}(x, \lambda, \xi) = 0 \qquad \text{in } \mathcal{D},$$

$$(2.7) \qquad\qquad\qquad\qquad\qquad \nabla \cdot \tilde{u}(x, \lambda, \xi) = 0 \qquad \text{in } \mathcal{D},$$

$$(2.8) \qquad\qquad\qquad\qquad\qquad \tilde{u}(x, \lambda, \xi) = g(x, \lambda, \xi) \qquad \text{on } \Gamma,$$

$$(2.9) \qquad\qquad\qquad \tilde{u}(x, \lambda = 0, \xi) = u_I(x, \xi) \qquad \text{in } \mathcal{D}$$

almost surely in $\Omega$. Note that the velocity and pressure variables have been redefined by

$$(2.10) \qquad \tilde{u}(x, t/T(\xi), \xi) := u(x, t, \xi), \quad \tilde{p}(x, t/T(\xi), \xi) := T(\xi)p(x, t, \xi).$$

In the following the tilde notation will be dropped for notational convenience.

**2.3. Discretization and variational formulation.** The discretization of the probability space is carried out by means of a basis of orthonormal stochastic polynomials in $\xi$. Specifically, the velocity and pressure fields $u, p$ are approximated by their finite PC expansion:

$$[u(x, \lambda; \xi), p(x, \lambda; \xi)] = \sum_{i=0}^{P} [u_i(x, \lambda), p_i(x, \lambda)]\psi_i(\xi).$$

Here, the truncation parameter $P$ satisfies $(P + 1) = (p + L)!/p!L!$, where $p \in \mathbb{N}$ is the maximum total polynomial degree of the normalized chaos polynomials $\psi_i$, $i = 0, 1, 2, \ldots$. Their specific polynomials $\psi_i$ depends on the probability distribution of $\xi$ through the orthonormality condition. For instance, if $\xi$ is Gaussian then the PC expansion uses Hermite polynomials which are orthogonal with respect to the Gaussian measure. Other chaos polynomials are defined accordingly for other types of probability distributions, see, for example, [34, 15].

For notational convenience, we shall denote by $\mathcal{S}^P$ the subspace of $\mathcal{S}$ spanned by the PC basis.

Next, the PC discretizations are inserted into the scaled Navier–Stokes equations (2.6)–(2.9), which are then projected onto $\mathcal{S}^P$, resulting in

$$\partial_\lambda u_k(x, \lambda) + \sum_{j=0}^{P}\sum_{l=0}^{P}(u_j(x, \lambda) \cdot \nabla)u_l(x, \lambda)c(T)_{jlk}$$

$$(2.11) \qquad\qquad - \sum_{j=0}^{P}\Delta u_j(x, \lambda)\nu(T)_{jk} + \nabla p_k(x, \lambda) = 0 \qquad \text{in } \mathcal{D},$$

$$(2.12) \qquad\qquad\qquad\qquad\qquad\qquad \nabla \cdot u_k(x, \lambda) = 0 \qquad \text{in } \mathcal{D},$$

$$(2.13) \qquad\qquad\qquad\qquad\qquad\qquad u_k(x, \lambda) = \langle g, \psi_k \rangle \qquad \text{on } \Gamma,$$

$$(2.14) \qquad\qquad\qquad\qquad\qquad u_k(x, \lambda = 0) = \langle u_I, \psi_k \rangle \quad \text{in } \mathcal{D}$$

for $\lambda > 0$ and $k = 0, \ldots, P$. The angle brackets $\langle \cdot, \cdot \rangle$ denote the inner product on $\mathcal{S}$, and the third and second order tensors are defined by

$$c(T)_{jlk} := \sum_{i=0}^{Q} T_i \langle \psi_i \psi_j \psi_l, \psi_k \rangle, \quad \nu(T)_{jk} := \nu \sum_{i=0}^{Q} T_i \langle \psi_i \psi_j, \psi_k \rangle$$

for $j, l, k = 0, \ldots, P$. For the period $T$, we again rely on a PC expansion, truncated to a maximum total polynomial degree $q$, so that

$$T(\xi) = \sum_{i=0}^{Q} T_i \psi_i(\xi), \quad Q + 1 = \frac{(q + L)!}{q!L!}.$$

We consistently denote $\mathcal{S}^Q$ the corresponding subspace of $\mathcal{S}$.

Note that both tensors have many zero valued entries, especially when eventually a low order expansion for $T$ will be employed. This significantly reduces the number of coupling terms in (2.11). Furthermore, the redefinition of the pressure variable in (2.10) plays an important role, since the pressure term appears completely decoupled in (2.11), which would not be the case if the pressure term would still involve a product with the stochastic period $T(\xi)$, as is the case for the viscosity term. However, the number of coupling terms within (2.11) is significantly increased in comparison to a Galerkin projection of the standard unscaled formulation (2.1) due to the nonlinear convective term.

A variational formulation (at the deterministic level) of the stochastic Galerkin system (2.11)–(2.14) is the following.

For $k = 0, \ldots, P$, $\lambda > 0$, and given period modes $T_k$, find $u_k(\cdot, \lambda) \in V$ and $p_k(\cdot, \lambda) \in W$ such that for all $v \in V_0$, for all $q \in W$,

$$(2.15) \qquad (\partial_\lambda u_k, v) + \sum_{j,l=0}^{P} ((u_j \cdot \nabla)u_l, v)c(T)_{jlk} + \sum_{j=0}^{P} (\nabla u_j, \nabla v)\nu(T)_{jk} - (p_k, \nabla \cdot v) = 0,$$

$$(2.16) \qquad\qquad\qquad\qquad\qquad\qquad\qquad\qquad\qquad (\nabla \cdot u_k, q) = 0,$$

$$(2.17) \qquad\qquad\qquad\qquad\qquad\qquad\qquad\qquad u_k(x, \lambda) = \langle g, \psi_k \rangle \quad \text{on } \Gamma,$$

$$(2.18) \qquad\qquad\qquad\qquad\qquad\qquad\qquad u_k(x, \lambda = 0) = \langle u_I, \psi_k \rangle \quad \text{in } \mathcal{D}.$$

Here, $(\cdot, \cdot)$ denotes the inner product on $W$. We solve the coupled system (2.15)–(2.18) by means of a classical finite element method with finite-dimensional spaces $V^h \subset V$ and $W^h \subset W$. For an overview on existing finite element solvers for the deterministic Navier–Stokes equations see, e.g., [6, 7, 10, 31]. For solving and preconditioning (2.15)–(2.18) see, e.g., [14, 16, 20, 23, 24].

**2.4. Determining the period and initial condition.** We define the following operator to track the velocity as a function of the scaled time variable $\lambda \geq 0$ subject to some period $T$ and initial condition $u_I$:

$$(2.19) \qquad\qquad \mathcal{U}(u_I, T, \lambda) := u_I + \int_0^\lambda \partial_\lambda u(\lambda = \sigma) \, d\sigma,$$

where $u$ satisfies (2.15)–(2.18). Note that $\mathcal{U}$ represents the velocity at time $\lambda$ starting from the initial condition $u_I$, whose PC expansion will be denoted by

$$(2.20) \qquad\qquad \mathcal{U}(u_I, T, \lambda) = \sum_{i=0}^{P} \mathcal{U}_i(u_I, T, \lambda)\psi_i,$$

where $\mathcal{U}_i \in V$ for $i = 0, \ldots, P$, such that $\mathcal{U}_i = \mathcal{U}_i(u_I, T, \lambda)(x) = u_i(x, \lambda)$ with $u_i$ denoting the $i$-th mode of the PC expansion of the velocity $u$ satisfying (2.15)–(2.18) at time $\lambda$.

The problem definition of finding almost surely time-periodic solutions to the S-SNSE can be formulated in the following way.

Find some $u_I$, whose PC coefficients satisfy (2.16)–(2.17), and a corresponding $T$ as in Assumption 1, such that

$$(2.21) \qquad\qquad\qquad \|\mathcal{U}(u_I, T, 1) - u_I\|^2 = 0,$$

where here and for the rest of this work $\|\cdot\| := \|\cdot\|_{\mathcal{S}\otimes W}$. Because of the truncation error, (2.21) can be formally satisfied only if $u_I \in \mathcal{S}^P \otimes V$; otherwise a weak interpretation can be invoked. Note that the determination of the period $T$ imposes an additional constraint on the S-SNSE. Therefore, we suggest an iterative approach, which will be explained in detail within the following section.

**3. Solution procedure.** In the following an iterative method, inspired by an approach for deterministic problems introduced by Duguet, Pringle, and Kerswell [4], will be described for computing an initial condition $u_I$ and a period $T$ satisfying (2.21), employing Newton's method, the solution of an optimization problem, and an optimality based *phase controlling*. The initial condition is sought in $\mathcal{S}^P \otimes V$, while a stochastic discretization of the period is needed.

For $\lambda \geq 0$ and some initial condition $u_I$ we define a distance vector $D$ by

$$D(u_I, T, \lambda) := u_I - \mathcal{U}(u_I, T, \lambda).$$

Therefore, $\|D\|$ measures the distance between an initial condition $u_I$ and its state $\mathcal{U}(u_I, T, \lambda)$ at time $\lambda$. The goal of the iteration procedure is to obtain convergence such that

$$\|D(u_I^k, T^k, \lambda)\| \to 0 \quad \text{as } k \to \infty.$$

We start by choosing some appropriate initial guesses $u_I^0 = \sum_{i=0}^{P} u_{I,i}^0 \psi_i$ and $T^0 = \sum_{i=0}^{Q} T_i^0 \psi_i$ for the initial condition and period, respectively. As an initial guess for $u_I^0$ and corresponding $T^0$ we suggest using a fully developed deterministic flow, i.e., $u_{I,i}^0 = 0$ and $T_i^0 = 0$ for $i > 0$, which has been computed a priori by integration of the deterministic Navier–Stokes equations parametrized by the mean of the random input.

**3.1. An optimality constraint for determining the period.** To arrive at an update formula for the period, we first define an optimization problem, which ensures that the distance between the initial condition and its terminal state remains minimal in an $L^2$-sense (cf. Figure 1. Therefore, given the $k$-th iterates $u_I^k$ and $T^k$, we aim at correcting the period $T^k$ through

$$(3.1) \qquad\qquad T^{k+1} = (1 + d\lambda)T^k \approx \sum_{m=0}^{Q} T_m^{k+1} \psi_m,$$

$$(3.2) \qquad\qquad T_m^{k+1} = T_m^k + \sum_{i=0}^{Q}\sum_{j=0}^{Q} d\lambda_i T_j^k \langle \psi_i \psi_j, \psi_m \rangle, \quad m = 0, \dots, Q,$$

where we employed a Galerkin projection using the PC expansion of $d\lambda \in \mathcal{S}^Q$, which is a solution of the minimization problem

$$(3.3) \qquad\qquad \min_{d\lambda \in \mathcal{S}^Q} \|u_I^k - \mathcal{U}(u_I^k, T^k, 1 + d\lambda)\|^2.$$
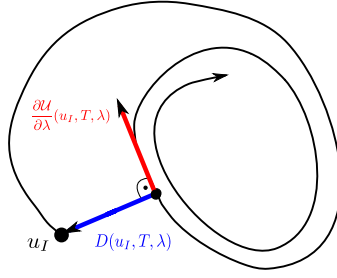
**Figure 1.** *Schematic view of a trajectory starting at some initial condition $u_I$ with distance vector $D$ and time derivative $\frac{\partial \mathcal{U}}{\partial \lambda}$ for some realization of $\xi$.*

To simplify problem (3.3), we approximate $\mathcal{U}(u_I^k, T^k, 1 + d\lambda)$ by its first order Taylor series representation around $\lambda = 1$, i.e.,

$$(3.4) \qquad \mathcal{U}(u_I^k, T^k, 1 + d\lambda) \approx \mathcal{U}(u_I^k, T^k, 1) + \partial_\lambda \mathcal{U}(u_I^k, T^k, 1)d\lambda.$$

Inserting (3.4) in (3.3) results in a linearized stochastic optimization problem for the correction term $d\lambda$:

$$(3.5) \qquad \min_{d\lambda \in \mathcal{S}} \|D(u_I^k, T^k, 1) - \partial_\lambda \mathcal{U}(u_I^k, T^k, 1)d\lambda\|^2.$$

The corresponding optimality condition reads as

$$(3.6) \qquad 2\left\langle \left( D(u_I^k, T^k, 1) - \partial_\lambda \mathcal{U}(u_I^k, T^k, 1)d\lambda, \partial_\lambda \mathcal{U}(u_I^k, T^k, 1) \right) \right\rangle = 0.$$

Introducing the PC expansions of the various stochastic quantities into (3.6) we arrive at the discrete optimality condition for the PC modes $\vec{d\lambda} = [d\lambda_0, \ldots, d\lambda_Q]^t \in \mathbb{R}^{Q+1}$:

$$(3.7) \qquad A\,\vec{d\lambda} = b,$$

where $A \in \mathbb{R}^{Q+1,Q+1}$ and $b \in \mathbb{R}^{Q+1}$ are defined by

$$A_{ml} := \sum_{i,j=0}^{P} \langle \psi_i \psi_j \psi_l, \psi_m \rangle (\partial_\lambda \mathcal{U}_i^k, \partial_\lambda \mathcal{U}_j^k), \quad b_m := \sum_{i,j=0}^{P} \langle \psi_i \psi_j, \psi_m \rangle (D_i^k, \partial_\lambda \mathcal{U}_j^k)$$

for $m, l = 0, \ldots, Q$. The corresponding PC coefficients of $\partial_\lambda \mathcal{U}$ and $D$ are given by

$$\partial_\lambda \mathcal{U}_i^k = \langle \partial_\lambda \mathcal{U}(u_I^k, T^k, 1), \psi_i \rangle, \quad D_i^k = \langle D(u_I^k, T^k, 1), \psi_i \rangle$$

for $i = 0, \ldots, P$.

**Lemma 3.1.** *The optimization problem (3.5) for $d\lambda = \sum_{i=0}^{Q} d\lambda_i \psi_i$ is convex.*

*Proof.* We show that the Hessian of the optimization problem is positive semidefinite. For notational convenience, $\dot{\mathcal{U}}^k$ and $D^k$ are defined by $\dot{\mathcal{U}}^k := \partial_\lambda \mathcal{U}(u_I^k, T^k, 1)$ and $D^k :=$

$D(u_I^k, T^k, 1)$. We determine the second partial derivatives of (3.5) with respect to $d\lambda_m$ and $d\lambda_n$, $n, m = 0, \ldots, Q$:

$$h_{mn} := \frac{\partial^2}{\partial d\lambda_n \partial d\lambda_m} \left\| D^k - \dot{\mathcal{U}}^k \sum_{l=0}^{P} d\lambda_l \psi_l \right\|^2 = 2\langle (\dot{\mathcal{U}}^k \psi_n, \dot{\mathcal{U}}^k \psi_m) \rangle,$$

which defines the Hessian $H := (h_{mn})_{m,n=0}^{Q}$. Let $y = [y_0, \ldots, y_Q]^t \in \mathbb{R}^{Q+1}$, $y \neq 0$, be arbitrary; then the following relations hold:

$$y^t H y = 2 \sum_{m,n=0}^{Q} y_m \langle (\dot{\mathcal{U}}^k \psi_n, \dot{\mathcal{U}}^k \psi_m) \rangle y_n = 2 \left\| \sum_{m=0}^{Q} y_m \psi_m \dot{\mathcal{U}}^k \right\|^2 \geq 0.$$

Therefore, $H$ is positive semidefinite, which completes the proof. ∎

Summing up, the determination of the new period update $T^{k+1}$ via (3.1) requires the solution of one or several linear systems of equations, as stated in (3.7), which can be carried out by employing standard direct numerical solvers.

*Remark* 1. Note that, because of the linearization error in (3.4), iterations on the period correction can reduce the overall error in (2.21) significantly. For these iterations, after the period has been updated through (3.1), to say $T^*$, the corresponding terminal state $\mathcal{U}(u_I, T^*, 1)$ is recomputed for the same initial condition $u_I^k$ and used to determine the subsequent correction $d\lambda$. The iterations are stopped whenever $d\lambda$ becomes small enough and finally $T^{k+1} = T^*$.

**3.2. Newton's method for updating the initial condition.** Updating the period iterate ensures that the terminal state has a minimal distance with respect to the current initial condition iterate $u_I^k$. In general the minimum is greater than zero, which necessitates a correction of $u_I^k$ such that the distance can be decreased further.

This is achieved by applying Newton's method to $D(u_I^k, T^{k+1}, 1) = 0$. The corresponding Newton step reads as

$$(3.8) \qquad u_I^{k+1} = u_I^k + du_I^k, \quad -J_k[du_I^k] = D(u_I^k, T^{k+1}, 1),$$

where $J_k[du_I^k]$ denotes the Jacobian of $D(u_I, T^{k+1}, 1)$ with respect to $u_I$ in direction $du_I^k$ at $u_I = u_I^k$. Due to the large system size, solving the linear system in (3.8) should be carried out by using iterative solvers, e.g., by the generalized minimal residual method (GMRES method [26]) suitable for non-symmetric systems. Note that to reduce the computational cost an inexact Newton approach should be used such that a low accuracy for solving the linear system in (3.8) is sufficient enough to achieve overall convergence; see, e.g., [5]. The following section provides a detailed analysis on solving (3.8).

**3.3. Solving the Newton step.** For each iteration during the solution of (3.8), represented by some iterate $w$, the "effect" of the Jacobian $J_k[w]$ has to be evaluated. This can be carried out by solving the linearized Navier–Stokes equations, which will be elaborated on in the following.

First we note that the application of the Jacobian $J_k$ to some $w$ can further be simplified by

$$J_k[w] = w - J_k^{NS}[w],$$

by definition of $D$, where $J_k^{NS}$ denotes the Jacobian of the terminal state $\mathcal{U}(u_I^k, T^{k+1}, 1)$ in direction $w$. Therefore, the focus is shifted towards the computation of $J_k^{NS}[w]$, which for the following analysis will be denoted by $J[w]$ for notational convenience. Furthermore, to simplify the derivation of the linear model, divergence-free vector spaces for the velocity $u$ arising from the S-SNSE are assumed such that the pressure variable can be neglected. Also, the strong formulation of the S-SNSE is being considered, provided that the velocity variable fulfills the regularity requirements of a classical solution to the stochastic Navier–Stokes equations. In an analogous yet more technical way, the results of this section can be transferred to the mixed-type variational formulation involving the pressure variable with fewer regularity requirements on the velocity $u$.

We define the Navier–Stokes operator $F$ by

$$F(u_I, u) := \begin{bmatrix} \partial_\lambda u + T(u \cdot \nabla)u - \nu T \Delta u \\ u_{|\Gamma} - g \\ u(\lambda = 0) - u_I \end{bmatrix}$$

such that $F(u_I, u) = 0$ represents the S-SNSE in their strong formulation subject to a Dirichlet condition $g$. Furthermore, let $u_I^* := u_I^k$; then there exists a solution $u^*$ such that $F(u_I^*, u^*) = 0$ [25, 30]. It can be shown that $F$ is $C^\infty$-differentiable [13] in a neighborhood of $(u_I^*, u^*)$. The directional Gâteaux derivative of $F$ with respect to $u$ in direction $\bar{u}$ can be easily calculated and reads as

$$F_u(u_I, u)[\bar{u}] = \begin{bmatrix} \partial_\lambda \bar{u} + T(\bar{u} \cdot \nabla)u + T(u \cdot \nabla)\bar{u} - \nu T \Delta \bar{u} \\ \bar{u}_{|\Gamma} \\ \bar{u}(\lambda = 0) \end{bmatrix}.$$

Assuming that the partial Fréchet derivative $F_u$ is bijective in a neighborhood of $(u_I^*, u^*)$ allows the use of the implicit function theorem [35], from which it follows that

$$(3.9) \qquad -F_u(u_I, u)u'(u_I) = F_{u_I}(u_I, u)$$

for all $(u_I, u)$ in a neighborhood of $(u_I^*, u^*)$. Note that $u'(u_I)[w] = J[w]$ for a direction $w$. Therefore, inserting this relation into (3.9) at $(u_I, u) = (u_I^*, u^*)$ with respect to the direction $w$ yields

$$(3.10) \qquad -\begin{bmatrix} \partial_\lambda v + T(v \cdot \nabla)u^* + T(u^* \cdot \nabla)v - \nu T \Delta v \\ v_{|\Gamma} \\ v(\lambda = 0) \end{bmatrix} = \begin{bmatrix} 0 \\ 0 \\ -w \end{bmatrix}$$

for $v := J[w]$.

Summing up, the computation of the directional derivative $J[w]$ of the terminal state $\mathcal{U}(u_I^k, T^{k+1}, 1)$ with respect to $u_I$ in direction $w$ does not require a solution of the nonlinear form of the S-SNSE. Instead, given an iterate $u_I^k$ and its corresponding terminal state $\mathcal{U}(u_I^k, T^{k+1}, 1)$, it suffices to solve a linearized version of the S-SNSE subject to homogeneous Dirichlet boundary conditions on the boundary $\Gamma \subset \partial \mathcal{D}$ and initial condition $w$, with linearization around the trajectory of the velocity between the initial condition $u_I^k$ and its terminal

state $\mathcal{U}(u_I^k, T^{k+1}, 1)$ as stated in (3.10). The weak mixed-type formulation, i.e., with consideration of the pressure variable, results in a non-symmetric system, solution of which can be computed, for example, by applying GMRES as an iterative inner-loop solver again.

*Remark* 2. Note that, instead of solving the linearized equations, it is also possible to approximate the Jacobian by a finite difference scheme [4], which, however, would require solving the nonlinear version of the S-SNSE in each iteration.

**3.4. Phase-drift control.** Having computed some initial condition iterate $u_I^k$, it is possible that the trajectories corresponding to different realizations of the random input $\xi$ deviate too much such that an increasing polynomial degree needs to be employed to capture the stochastic variations. This is due to the arbitrariness of the stochastic phase on the initial condition definition. Indeed, if $u_I(\xi)$ is a valid initial condition, in the sense that it belongs (almost surely) to the stochastic limit-cycle having a period $T(\xi)$, then $\mathcal{U}(u_I, T(\xi), \beta(\xi))$ is another valid initial condition for all $\beta(\xi) > 0$. This can cause numerical instabilities of the algorithm, and iterations need to be controlled in an appropriate way. Therefore, we define a control step which ensures that the trajectories remain essentially *in-phase*. This control is based on the ideas initially proposed in [18].

The *phase-drift* can be measured with respect to a deterministic reference trajectory. To this end, we define a reference $\hat{u}$ as the velocity evaluated at the mean $\bar{\xi}$ of the random input, i.e.,

$$\hat{u}(\lambda, x) := u(\lambda, x, \xi)|_{\xi=\bar{\xi}}.$$

The distance between the stochastic velocity field and the reference is defined by

$$\delta u(\lambda, x, \xi) := u(\lambda, x, \xi) - \hat{u}(\lambda, x)$$

such that the *phase-drift* can be measured by the weighted inner product $\Sigma(\lambda, \xi)$ of the distance and the time tangential of the stochastic velocity field:

$$\Sigma(\lambda, \xi) := \frac{(\delta u, \partial_\lambda \hat{u})}{(\partial_\lambda \hat{u}, \partial_\lambda \hat{u})^{1/2}}.$$

Note that $(\partial_\lambda \hat{u}, \partial_\lambda \hat{u}) > 0$ in an almost surely unsteady flow. An *in-phase* condition is equivalent to minimizing $\Sigma(\lambda, \xi)$ in some sense, which will be elaborated on in the following. Therefore, in addition to the time scaling by the period $T$, we introduce a further stochastic time scaling $\tau$, modifying the time scale $\lambda$ by

$$\tau(t, \xi) := \frac{\lambda(t, \xi)}{\sigma(t, \xi)},$$

where $\sigma$ is defined to be an almost surely positive random process, which is piecewise constant in the physical time scale $t$ with respect to some finite number of time intervals. Suppose we employ some time discretization scheme of $\lambda$, denoted by some function $h$, such that

$$u^{n+1} = u^n + h(\Delta\lambda, u^n, u^{n+1}, \xi),$$

where $u^n := u(\lambda^n)$ and $\Delta\lambda > 0$ denotes a (deterministic) time step size, which can be defined, for example, by

$$\Delta\lambda := \frac{\Delta t}{T(\bar{\xi})} > 0$$

for $\Delta t > 0$. Introducing the new stochastic time scaling $\sigma$, we get

$$u^{n+1} = u^n + \sigma(\xi)h(\Delta\lambda, u^n, u^{n+1}, \xi),$$

due to $\sigma$ being piecewise constant in $t$. Therefore, we obtain the possibility of modifying each time stepping for every trajectory resulting from a realization of $\xi$. The remaining question is how to define the time scaling $\sigma$. Note that $\sigma := 1$ corresponds to no additional time scaling but $\lambda$.

In this work we employ a simple heuristic to control the behavior of $\sigma$ within each time interval. For this purpose we monitor the quantity $\Sigma(\lambda, \xi)$ and define the "rule":

$$\sigma(\xi) < 1 \quad \text{if } \Sigma > 0 \quad \text{(slow down)},$$
$$\sigma(\xi) > 1 \quad \text{if } \Sigma < 0 \quad \text{(speed up)}.$$

Therefore, a trajectory is sped up if the angle between the reference and the trajectory is greater than $\pi/2$, and it is slowed down in the other case. As a simple heuristic we define

$$\sigma(\xi) := \left(1 + \theta\frac{1}{\Delta\lambda}(\partial_\lambda u, \partial_\lambda u)\Sigma(\lambda, \xi)\right),$$

where $\theta > 0$ is some prescribed control parameter. Note that this heuristic does not necessarily guarantee an almost surely positive $\sigma$. However, for a sufficiently small $\theta$ it can be assumed that $\sigma$ remains close to 1, which, however, reduces the control influence of $\sigma$. Furthermore, if the trajectories are *in-phase*, $\sigma$ returns to 1 by definition.

The application of the control step is carried out with respect to one cycle subject to the current period iterate $T^k$. This requires the solution of the time scaled Navier–Stokes equations, where after completion of one cycle, we choose the velocity with a minimal $\Sigma$ along the computed trajectory as a new initial condition $u_I^k$. In our numerical applications, we chose $\theta$ to be the current norm of the distance between the initial condition iterate and its corresponding terminal condition (cf. (2.21)). A small distance suggests that the trajectories should be at least close to *in-phase* such that no additional phase correction should be necessary.

*Remark* 3. Note that if $\theta$ is chosen too large, then the control becomes numerically unstable, since the positivity constraint could be violated.

**3.5. The algorithm.** This section briefly recapitulates the algorithm introduced in the previous sections. As can be seen from Algorithm 1, the computation of a periodic orbit requires the solution of various Navier–Stokes problems in each iteration, which is certainly the bulk of the numerical cost. One iteration requires the solution of multiple nonlinear stochastic Navier–Stokes problems and multiple linearized stochastic Navier–Stokes problems. Therefore, the numerical efficiency of this algorithm strongly depends on the numerical efficiency on the available numerical solvers for the stochastic Navier–Stokes equations. Especially, in the context of high Reynolds number flows, a numerically stable finite element discretization along with the stochastic Galerkin projection requires a large number of degrees of freedom to capture all dynamics of the flow.

Note the the parameter $\gamma > 0$ allows a user control over the accuracy of the computed period iterate, which affects the convergence speed of the algorithm. In our computations shown in section 4 it was sufficient to choose $\gamma = 1.0$.

**Algorithm 1.** Computation of stochastic periodic orbits.

1: Choose initial guesses $u_I^0$ and $T^0$
2: Choose tolerances $\epsilon > 0$, $\gamma > 0$, and $k_{max} \in \mathbb{N}$
3: $k \leftarrow 0$
4: Compute terminal condition $u_T^0 \leftarrow \mathcal{U}(u_I^0, T^0, 1)$ (nonlinear stochastic NS)
5: $r^0 \leftarrow \|u_I^0 - u_T^0\| / \|u_I^0\|$
6: **while** $k < k_{max}$ **and** $r^k > \epsilon$ **do**
7:     $k \leftarrow k + 1$
8:     Correct initial condition $u_I^{k-1}$ by phase control (nonlinear stochastic NS)
9:     **while** $\|d\lambda\| > \gamma \|r^{k-1}\|$ **do**
10:        Compute $d\lambda = \sum_{i=0}^{M} d\lambda_i \psi_i$ (nonlinear stochastic NS)
11:        Update period modes $T_m^k \leftarrow T_m^{k-1} + \sum_{i=0}^{M} \sum_{j=0}^{Q} d\lambda_i T_j^{k-1} \langle \psi_i \psi_j, \psi_m \rangle, \quad m = 0, \ldots, Q$
12:     **end while**
13:     Compute terminal condition $u_T^k \leftarrow \mathcal{U}(u_I^{k-1}, T^k, 1)$ (nonlinear stochastic NS)
14:     Solve inexact Newton step $-J_k[du_I^k] = u_I^{k-1} - u_T^k$ (linear stoch. NS, multiple times)
15:     Update initial condition $u_I^k \leftarrow u_I^{k-1} + du_I^k$
16:     Compute terminal condition $u_T^k \leftarrow \mathcal{U}(u_I^k, T^k, 1)$ (nonlinear stochastic NS)
17:     $r^k \leftarrow \|u_I^k - u_T^k\| / \|u_I^k\|$
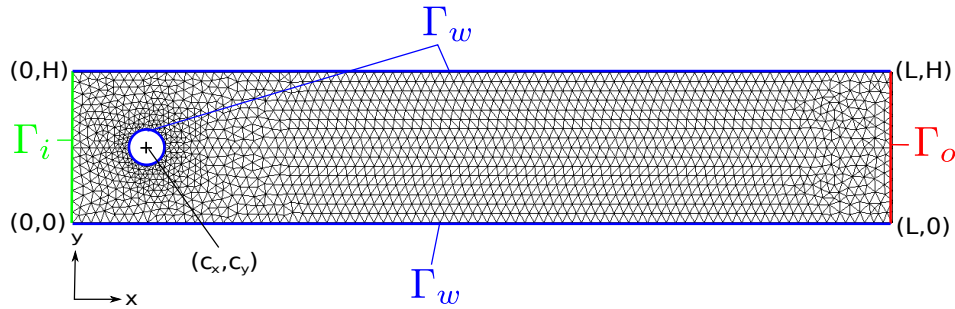18: **end while**
19: Post-processing



**Figure 2.** *Employed geometry and triangulation of a two-dimensional channel with a circular domain.*

**4. Numerical results.** The algorithm described in the previous section shall be verified employing a slightly modified benchmark problem originally introduced in [28]. It is a two-dimensional problem in the spatial variable, which describes a flow of an incompressible fluid around a circular domain within a channel of length $L$ and height $H$. Its exact geometrical data as well as the employed finite element mesh consisting of triangles is depicted in Figure 2 with $L = 2.2$, $H = 0.4$. The circular domain has a diameter of $D_c = 0.1$, and its center-point has the coordinates $(c_x, c_y) = (0.2, 0.2)$.

No-slip boundary conditions are considered for $\Gamma_w \subset \partial \mathcal{D} = (0, L) \times (0, H)$. The inflow

boundary condition at $\Gamma_i \subset \partial\mathcal{D}$ is set to be a stochastic parabolic profile, i.e.,

$$u_x(0, y, t; \xi) = 4v^{(1)}(\xi)y(H - y)/H^2$$

(4.1)
$$+ v^{(2)}(\xi)\sin(2\pi y/H), \quad y \in [0, H], \ t \geq 0,$$

(4.2)
$$u_y(0, y, t; \xi) = 0, \quad t \geq 0,$$

with $u = [u_x, u_y]$ denoting the components in the x- and y-directions of the velocity $u$, respectively. In the following sections, a one-dimensional and a two-dimensional uniformly distributed random input $\xi$ will be considered, where $v^{(1)}(\xi)$ and $v^{(2)}(\xi)$ will be defined later according to the numerical examples. For the outflow boundary condition at $\Gamma_o \subset \partial\mathcal{D}$ so-called do-nothing boundary conditions are applied [12]. These represent natural boundary conditions arising from the weak formulation of the SNSE by requiring all boundary integrals at $\Gamma_o$ to vanish in their sum, i.e.,

$$\int_{\Gamma_o} \nabla u_i \cdot \vec{n} - p_i\vec{n} \ dx = 0, \quad i = 0, \ldots, P,$$

where $u_i$ and $p_i$, $i = 0, \ldots, P$, denote the PC modes of the velocity and pressure variable, respectively, and $\vec{n}$ denotes the outward unit normal vector on the boundary $\Gamma_o$. Since this boundary condition results in a unique pressure variable, no additional requirements, such as $\int_{\mathcal{D}} p \ dx = 0$, are necessary.

For time integration a Crank–Nicolson scheme with a homogeneous time step size $\Delta t = 0.01$ for the unscaled time variable $t$ is employed. The corresponding time step length $\Delta\lambda > 0$ for the scaled time variable $\lambda$ is defined by

$$\Delta\lambda := \frac{\Delta t}{T^k(\xi = \bar{\xi})}.$$

Therefore, the time step size can vary for each iteration $k$ of the algorithm, depending on the value $T^k(\bar{\xi})$ of the period iterate. The spatial variable is discretized employing the finite element mesh depicted in Figure 2 and stable Taylor–Hood elements of order 2 for each stochastic mode of the velocity variable and order 1 for each pressure mode. The computations are carried out using the finite element software *HiFlow*[3] [1].

Furthermore, the kinematic viscosity $\nu$ is deterministic and set to $\nu = 0.001$ for all benchmark computations. The Reynolds number is calculated by

$$Re(\xi) = \frac{2}{3}\frac{v^{(1)}(\xi)D_c}{\nu}.$$

In the following numerical examples, we choose $v^{(1)}$ and $v^{(2)}$ such that a laminar time-periodic solution exists, which does not require any additional stabilization of the convective term. The flow is characterized by a periodic vortex shedding scheme behind the circular domain (the flow is considered from left to right; cf. Figure 2).

**4.1. One-dimensional random input.** In this section a one-dimensional random input $\xi \sim U(-1, 1)$, uniformly distributed in the interval $(-1, 1)$, is being considered. The random quantities $v^{(1)}(\xi)$ and $v^{(2)}(\xi)$ for the inflow boundary conditions (4.1) are set to

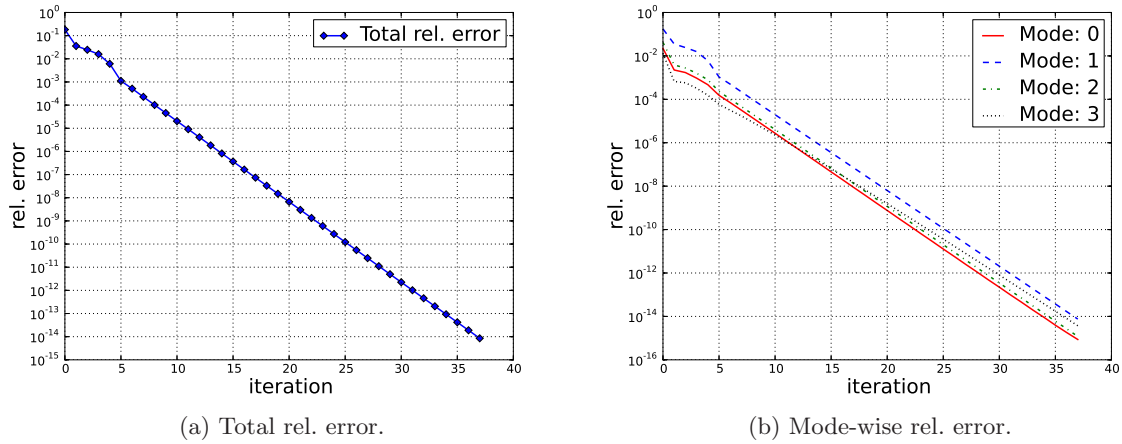$$v^{(1)}(\xi) := 1.5 + 0.15\xi, \quad v^{(2)}(\xi) := 0,$$

(a) Total rel. error.



(b) Mode-wise rel. error.

**Figure 3.** *Total and mode-wise relative error developments with respect to the number of iterations for a third order PC expansion.*

representing a stochastic parabolic inflow condition, which results in a uniformly distributed Reynolds number $Re \sim U(90, 110)$. Note that the uncertainty in the Reynolds number is introduced by the stochastic inflow condition only, since a deterministic viscosity $\nu = 0.001$ is used throughout the numerical computations.

We use a fully developed deterministic flow with corresponding deterministic period as an initial guess for the iteration procedure. For verification of the convergence properties of the algorithm we consider the relative errors based on the difference of the initial condition and its terminal state with respect to each iteration. Thereby, the total as well as the mode-wise relative errors are computed by the following relations:

$$\epsilon := \frac{\|u(\lambda = 1) - u(\lambda = 0)\|_{W \otimes \mathcal{S}^P}}{\|u^{final\ iteration}\|_{L^2((0,T) \times \mathcal{D} \times \Omega)}}, \quad \epsilon^i := \frac{\|u_i(\lambda = 1) - u_i(\lambda = 0)\|_W}{\|u^{final\ iteration}\|_{L^2((0,T) \times \mathcal{D} \times \Omega)}}.$$

The computations are carried out employing a third order Legendre PC expansion resulting in $P+1 = 4$ modes. As can be observed in Figure 3 the total as well as mode-wise relative errors decrease exponentially with respect to the number of iterations starting at the initial errors introduced by the initial guess up to machine precision. Furthermore, Figures 4(a) and 4(b) depict the absolute values and corresponding relative errors associated with the point-wise evaluation of the period computed by the PC expansion and corresponding deterministic sample computations. It can be observed that the period samples are approximated with an accuracy up to the order $O(10^{-3})$. We stress that the relation of the period $T(\xi)$ and $\xi$ is nonlinear, which is verified by estimating the probability density function of $T(\xi)$ (cf. Figure 4(c)). Figure 5(a) depicts the evolution of the *phase-drift*, measured by $\|\Sigma(\lambda, \xi)\|_{\mathcal{S}}$ (cf. section 3.4), during one cycle. It can be observed that the phase control keeps the trajectories in phase (in an $L^2$-sense), which stabilizes the numerical computation and allows for lower order PC expansions. Furthermore, we observe that the phase control exhibits a period with about twice the length of the period of the flow, which is due to the symmetry of the trajectories.
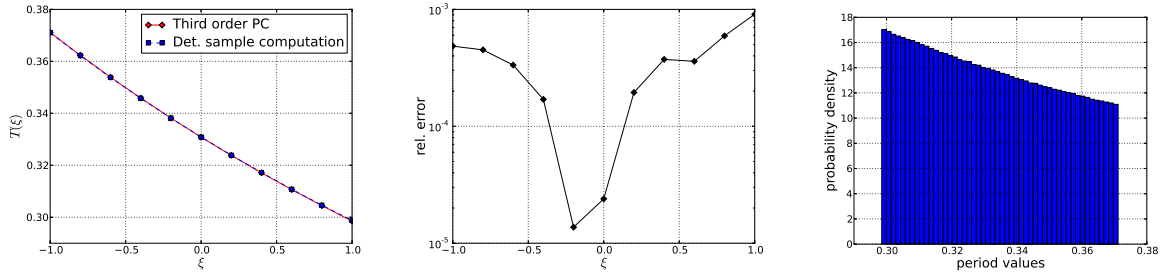
(a) Period values over input realizations.

(b) Relative error of period approximation.

(c) Estimation of period probability density function.

**Figure 4.** *Period approximation and probability density function estimation with absolute values and relative errors compared to deterministic simulations. A deterministic sample value corresponds to the period value computed by applying the algorithm on a deterministic system obtained by specific realizations of the random input $\xi$ at the plotted nodes. The "Third order PC" labelled period corresponds to the point evaluation of the PC expansion of the stochastic period.*
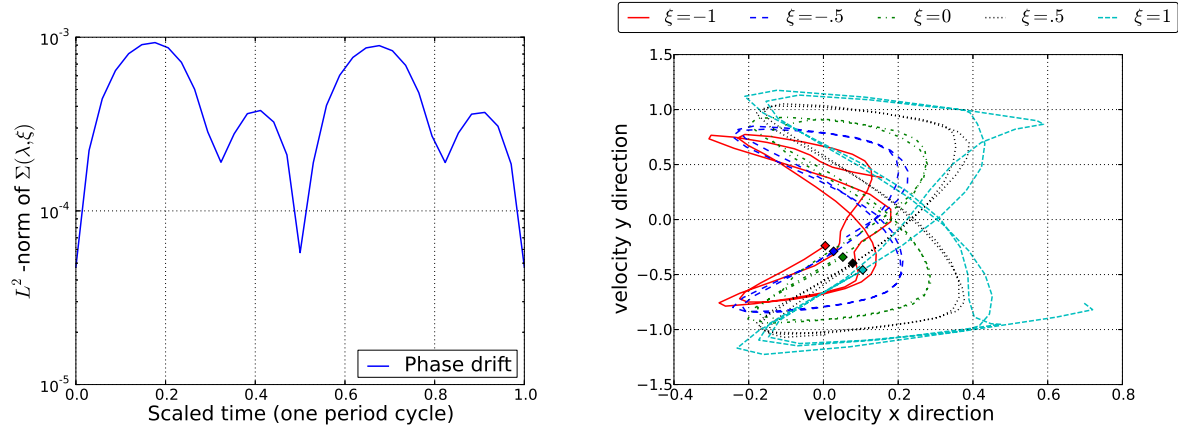


(a) Phase control during one limit-cycle.

(b) Convergence breakdown of standard Legendre chaos. Time evolution up to two period lengths for different realizations of $\xi$.

**Figure 5.** *Phase control and convergence breakdown of standard third order Legendre chaos.*

Figure 5(b) depicts a standard third order Legendre PC expansion computed by a straightforward time integration without employing the introduced algorithm. The standard approach leaves the limit-cycle after a very short time and is not able to complete even one cycle. This can be explained by an increasing *phase-drift* in the trajectories, which requires an increasing polynomial degree in time. Note that the introduced algorithm also employs a Legendre PC expansion due to the uniform distribution of the random input.

Although the decrease of the relative errors in Figure 3 suggests a high accuracy in computing the almost surely time-periodic limit-cycles of the trajectories, we verify the limit-cycles by a comparison of the stochastic PC approach and a purely deterministic reference simulation employing the same algorithm. The trajectories are depicted in Figure 6. It can be
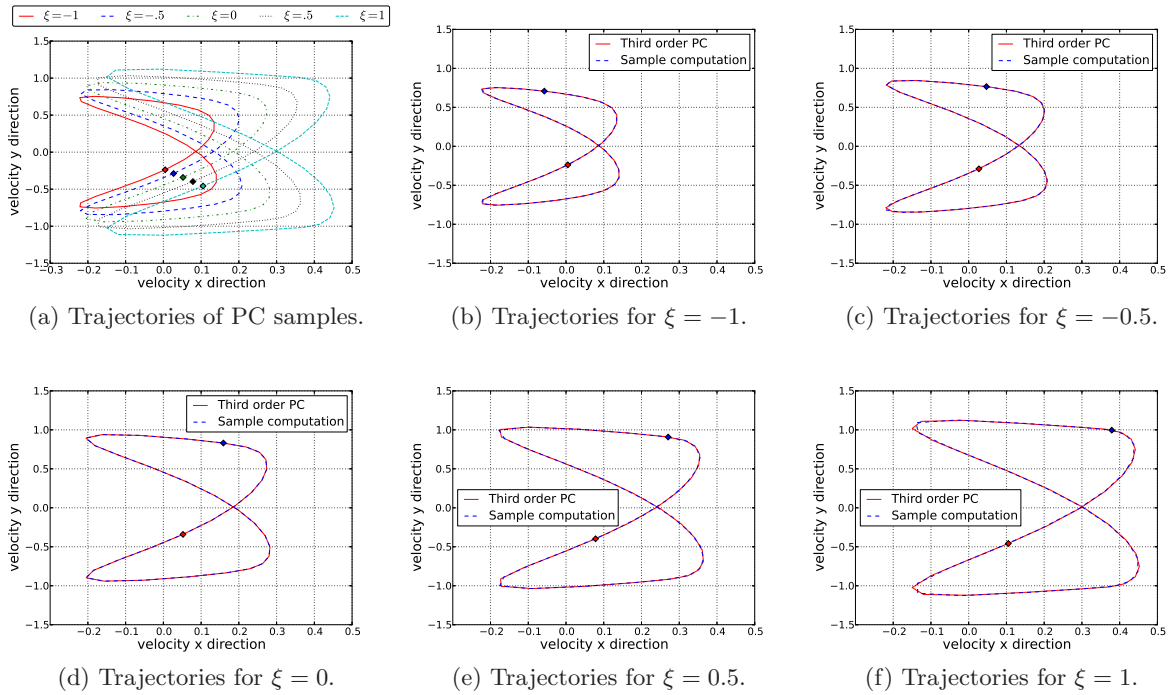
(a) Trajectories of PC samples.　　(b) Trajectories for $\xi = -1$.　　(c) Trajectories for $\xi = -0.5$.

(d) Trajectories for $\xi = 0$.　　(e) Trajectories for $\xi = 0.5$.　　(f) Trajectories for $\xi = 1$.

**Figure 6.** *Limit-cycles for PC solution and corresponding sample computations based on the solution of the deterministic reference systems obtained by a realization of the random input $\xi$.*
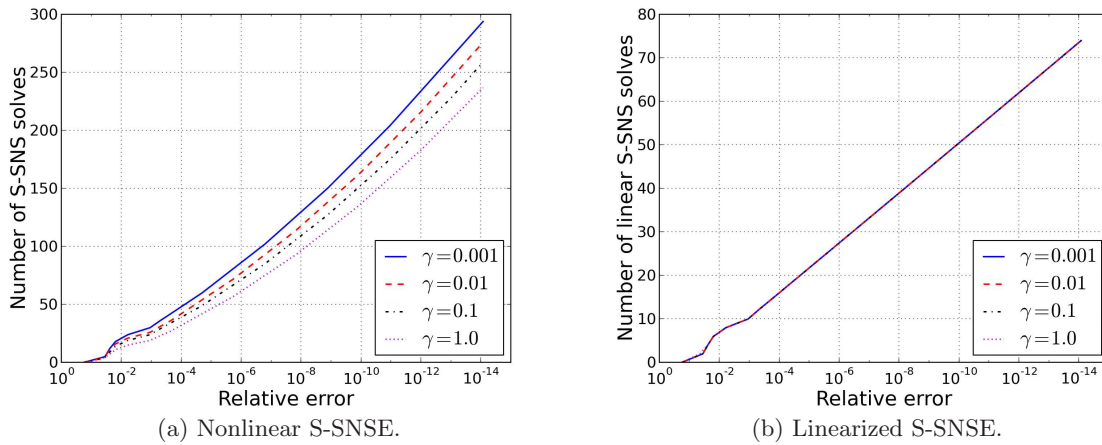


(a) Nonlinear S-SNSE.　　　　　　(b) Linearized S-SNSE.

**Figure 7.** *Required number of solves of the linearized and nonlinear S-SNSE with respect to desired accuracy and control parameter $\gamma$.*

observed that the dependence on $\xi$ has a significant impact on the shape and magnitude of the limit-cycles. Furthermore, there is a good agreement between the deterministic computations and the point evaluation of the PC solutions. In addition, the initial condition realizations at time $\lambda = 0$ are marked in the plots. Since the computations are carried out using an implicit time discretization scheme, the numerical stability allows for a large time step size resulting

in time steps varying between 30 and 38. Figure 7 depicts the required number of solves of the nonlinear S-SNSE as well as its linearized counterpart to achieve a certain relative error, where the value $\gamma = 1.0$ results in the least number of required solves. Achieving machine precision requires about 230 nonlinear and 75 linearized solves; in contrast, e.g., the solution up to the relative error of $10^{-4}$ requires about 30 nonlinear and 15 linearized solves. We stress that the numerical cost of the algorithm is proportional to the number of required S-SNSE solves. Overall, the numerical algorithm is capable of computing the stochastic limit-cycles with a high accuracy and overcomes the convergence breakdown of a standard PC expansion.

**4.2. Two-dimensional random input.** In this section the algorithm shall be applied to a more complex problem, characterized by a two-dimensional random input $\xi = (\xi_1, \xi_2)$, where $\xi_1, \xi_2 \sim U(-1, 1)$; i.e., we consider a two-dimensional independent uniformly distributed random vector in the interval $(-1, 1)$. The random quantities $v^{(1)}(\xi)$ and $v^{(2)}(\xi)$ for the inflow boundary conditions (4.1) are set to

$$v^{(1)}(\xi) := 1.5 + 0.15\xi_1, \quad v^{(2)}(\xi) := 0.15\xi_2,$$

representing a stochastic parabolic inflow condition with respect to $\xi_1$ and a stochastic sinus profile with respect to $\xi_2$. It is ensured that the inflow boundary condition remains positive almost surely.

The numerical computations are carried out up to a total relative error of order $O(10^{-9})$. We have observed that the period exhibits a dominant one-dimensional dependence on $\xi_1$. There is only a small dependence of the period on $\xi_2$ (not pictured). Therefore, the probability density exhibits a behavior similar to that for the one-dimensional random input case (cf. Figure 4(c)). Although $\xi_2$ has little effect on the period $T(\xi_1, \xi_2)$, the corresponding limit-cycles exhibit a significant dependence on both $\xi_1$ and $\xi_2$. This is verified by a comparison of deterministic reference scenarios and corresponding realizations of a third order Legendre PC solution in Figure 8. Furthermore, the results are compared to a first order Legendre PC expansion to demonstrate the dependence of the limit-cycle approximation on the order of the PC expansion. It can be observed that the third order expansion is capable of approximating each deterministic reference solution with high accuracy. In contrast, the first order expansion exhibits a significant deviation from the deterministic reference scenarios. However, this demonstrates the convergence with respect to the order of the PC expansion and stresses the importance of verifying the PC solutions according to their sample realizations. Figure 9 provides a summary of the different third order PC realizations to give a compact view on the dependence of the limit-cycles on the random inputs $\xi_1$ and $\xi_2$.

**5. Conclusions.** This paper is focused on the application of PC to fluid flow problems exhibiting stochastic limit-cycles, i.e., almost surely time-periodic solutions with uncertain period. A standard PC expansion is known to break down in convergence for this kind of problem because of strong nonlinear dynamics. This necessitates the development of appropriate numerical solvers overcoming the restrictions given by fixing a polynomial degree of a PC expansion. In this work, we introduce a numerical algorithm based on a reformulation of the governing equations by introducing the period as an unknown stochastic random variable to the unsteady incompressible Navier–Stokes equations subject to random input. This additional random variable is computed by an optimality constraint, which corrects the error
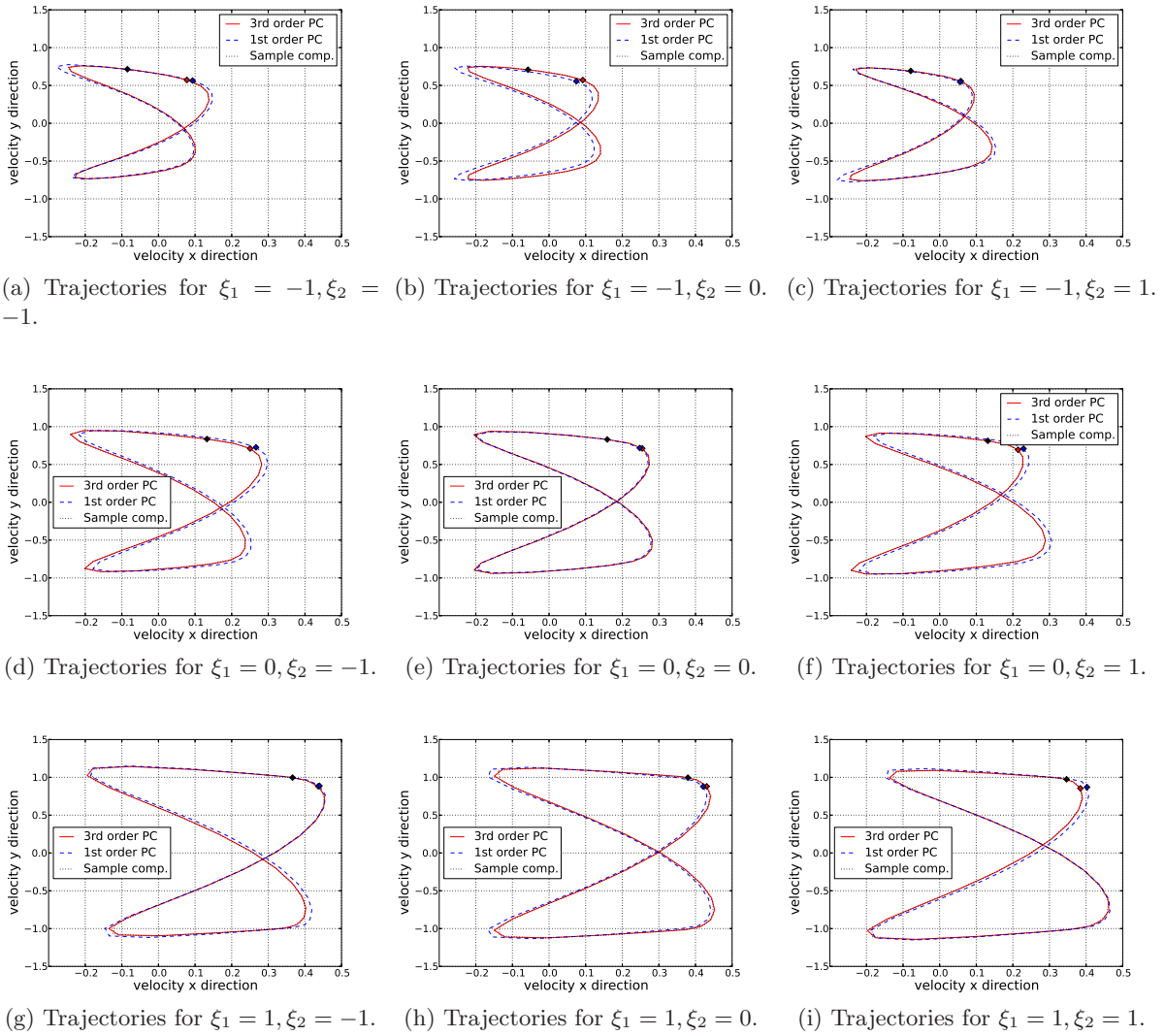
(a) Trajectories for $\xi_1 = -1, \xi_2 = -1$.

(b) Trajectories for $\xi_1 = -1, \xi_2 = 0$.

(c) Trajectories for $\xi_1 = -1, \xi_2 = 1$.

(d) Trajectories for $\xi_1 = 0, \xi_2 = -1$.

(e) Trajectories for $\xi_1 = 0, \xi_2 = 0$.

(f) Trajectories for $\xi_1 = 0, \xi_2 = 1$.

(g) Trajectories for $\xi_1 = 1, \xi_2 = -1$.

(h) Trajectories for $\xi_1 = 1, \xi_2 = 0$.

(i) Trajectories for $\xi_1 = 1, \xi_2 = 1$.

**Figure 8.** *Limit-cycles for PC solution and corresponding sample computations based on the solution of the deterministic reference systems obtained by a realization of the random input $\xi = (\xi_1, \xi_2)$.*
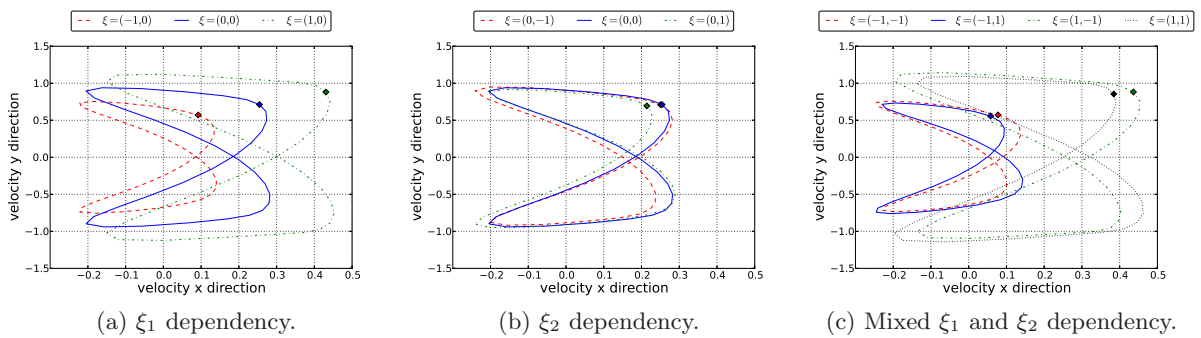


(a) $\xi_1$ dependency.

(b) $\xi_2$ dependency.

(c) Mixed $\xi_1$ and $\xi_2$ dependency.

**Figure 9.** *Point evaluation of limit-cycles of the third order PC solution.*

associated with the stochastic realizations of the period. Since a time-periodic solution can be characterized by a period and some corresponding initial condition of the flow at time $t = 0$, a Newton step is applied to provide an update formula for computing a new iterate of the initial condition. However, this does not automatically ensure that the trajectories corresponding to the realizations of the stochastic flow remain *in-phase* when integrating the governing equations in time. This can result in an increasing demand on the PC order to accurately approximate the initial condition. But since the initial condition is not unique, there exists another representative which requires a much lower expansion order, characterized by *in-phase* trajectories. Therefore, a stabilization step based on a heuristic optimization technique is introduced, which ensures that the trajectories remain *in-phase* when integrating in time.

The algorithm is applied to a benchmark problem representing a flow around a circular domain subject to a one- and a two-dimensional random input at the inflow boundary condition. For both cases excellent convergence results are achieved by employing a third order PC expansion. The algorithm itself exhibits an exponential convergence rate. Furthermore, the limit-cycles and the period are in very good agreement with deterministic reference solutions. However, one must pay attention to the employed order of the PC expansion. If a low PC expansion order is used, the solutions also follow a stochastic limit-cycle, but the trajectories are unable to capture the dynamics of the deterministic reference scenario, which requires an increase in the PC expansion order.

The numerical cost of the algorithm strongly depends on the employed numerical solvers for the solution of the stochastic Navier–Stokes equations, since these need to be solved multiple times during one iteration. Machine precision for the first benchmark problem was obtained by the solution of about 230 nonlinear S-SNSE and 75 linearized S-SNSE solves. The growth of the computational cost is exponential with respect to the achieved relative error. This is due to the linearization error arising from computing the period update, whose reduction results in a growing number of S-SNSE solves with respect to a prescribed relative error. Statistical properties of the random parameters, such as, for example, their mean, their variance, or their probability distribution, could theoretically have an effect on the convergence rate of the algorithm. A large stochastic variation in the period, for example, could result in more correction steps necessary for determining the period update.

The method outlined in this paper can be adapted to many other dynamical systems with uncertain parameters exhibiting stable limit-cycles. Indeed, the optimality constraint and the secondary time scaling are defined in a general way. The main effort in adapting the method to other types of dynamical systems concerns the non-linear Newton solver, as it requires the directional derivative of the solution (after one period of time) with respect to the initial state. Depending on the context and model considered, this Newton approach could be replaced by any available alternative, or even optimized as in [29] where a multiple shooting variant was developed for parallel-in-time computations.

## REFERENCES

[1] H. Anzt, W. Augustin, M. Baumann, T. Gengenbach, T. Hahn, A. Helfrich-Schkarbanenko, V. Heuveline, E. Ketelaer, D. Lukarski, A. Nestler, S. Ritterbusch, S. Ronnas,

M. Schick, M. Schmidtobreick, C. Subramanian, J.-P. Weiss, F. Wilhelm, and M. Wlotzka, *Hiflow*3: *A hardware-aware parallel finite element package*, in Tools for High Performance Computing 2011, H. Brunst, M. S. Müller, W. E. Nagel, and M. M. Resch, eds., Springer, Berlin, Heidelberg, 2012, pp. 139–151.

[2] P. S. Beran, C. L. Pettit, and D. R. Millman, *Uncertainty quantification of limit-cycle oscillations*, J. Comput. Phys., 217 (2006), pp. 217–247.

[3] B. M. Boghosian, L. M. Fazendeiro, J. Lätt, H. Tang, and P. V. Coveney, *New variational principles for locating periodic orbits of differential equations*, Philos. Trans. R. Soc. Lond. Ser. A Math. Phys. Eng. Sci., 369 (2011), pp. 2211–2218.

[4] Y. Duguet, C. C. T. Pringle, and R. R. Kerswell, *Relative periodic orbits in transitional pipe flow*, Phys. Fluids, 20 (2008), 114102.

[5] S. C. Eisenstat and H. F. Walker, *Choosing the forcing terms in an inexact Newton method*, SIAM J. Sci. Comput., 17 (1996), pp. 16–32.

[6] C. A. J. Fletcher, *Computational Techniques for Fluid Dynamics*, Vol. I, Springer Ser. Comput. Phys., Springer, Berlin, 1988.

[7] C. A. J. Fletcher, *Computational Techniques for Fluid Dynamics*, Vol. II, Springer Ser. Comput. Phys., Springer, Berlin, 1988.

[8] M. Gerritsma, J.-B. van der Steen, P. Vos, and G. E. Karniadakis, *Time-dependent generalized polynomial chaos*, J. Comput. Phys., 229 (2010), pp. 8333–8363.

[9] R. Ghanem and P. D. Spanos, *Stochastic Finite Elements: A Spectral Approach*, Springer-Verlag, New York, 1991.

[10] J. L. Guermond, P. Minev, and J. Shen, *An overview of projection methods for incompressible flows*, Comput. Methods Appl. Mech. Engrg., 195 (2006), pp. 6011–6045.

[11] V. Heuveline and M. Schick, *A hybrid generalized Polynomial Chaos method for stochastic dynamical systems*, Int. J. Uncertain. Quantif., 4 (2014), pp. 37–61.

[12] J. G. Heywood, R. Rannacher, and S. Turek, *Artificial boundaries and flux and pressure conditions for the incompressible Navier-Stokes equations*, Internat. J. Numer. Methods Fluids, 22 (1996), pp. 325–352.

[13] M. Hinze, R. Pinnau, M. Ulbrich, and S. Ulbrich, *Optimization with PDE Constraints*, Math. Model. Theory Appl. 23, Springer, New York, 2009.

[14] O. M. Knio and O. P. Le Maître, *Uncertainty propagation in CFD using polynomial chaos decomposition*, Fluid Dynam. Res., 38 (2006), pp. 616–640.

[15] O. P. Le Maître and O. M. Knio, *Spectral Methods for Uncertainty Quantification: With Applications to Computational Fluid Dynamics*, Springer, New York, 2010.

[16] O. P. Le Maître, O. M. Knio, H. N. Najm, and R. G. Ghanem, *A stochastic projection method for fluid flow*. I. *Basic formulation*, J. Comput. Phys., 173 (2001), pp. 481–511.

[17] O. P. Le Maître, O. M. Knio, H. N. Najm, and R. G. Ghanem, *Uncertainty propagation using Wiener-Haar expansions*, J. Comput. Phys., 197 (2004), pp. 28–57.

[18] O. P. Le Maître, L. Mathelin, O. M. Knio, and M. Y. Hussaini, *Asynchronous time integration for polynomial chaos expansion of uncertain periodic dynamics*, Discrete Contin. Dyn. Syst., 28 (2010), pp. 199–226.

[19] O. P. Le Maître, H. N. Najm, R. G. Ghanem, and O. M. Knio, *Multi-resolution analysis of Wiener-type uncertainty propagation schemes*, J. Comput. Phys., 197 (2004), pp. 502–531.

[20] O. P. Le Maître, M. T. Reagan, H. N. Najm, R. G. Ghanem, and O. M. Knio, *A stochastic projection method for fluid flow*. II. *Random process*, J. Comput. Phys., 181 (2002), pp. 9–44.

[21] O. P. Le Maître, M. T. Reagan, B. J. Debusschere, H. N. Najm, R. G. Ghanem, and O. M. Knio, *Natural convection in a closed cavity under stochastic, non-Boussinesq conditions*, SIAM J. Sci. Comp., 26:2 (2004), pp. 375-394.

[22] H. N. Najm, *Uncertainty quantification and polynomial chaos techniques in computational fluid dynamics*, Ann. Rev. of Fluid Mechanics, 41 (2009), pp. 35–52.

[23] C. E. Powell and D. J. Silvester, *Preconditioning steady-state Navier–Stokes equations with random data*, SIAM J. Sci. Comput., 34 (2012), pp. A2482–A2506.

[24] C. E. Powell and E. Ullmann, *Preconditioning stochastic Galerkin saddle point systems*, SIAM J. Matrix Anal. Appl., 31 (2010), pp. 2813–2840.

[25] A. QUARTERONI AND A. VALLI, *Numerical Approximation of Partial Differential Equations*, Springer Ser. Comput. Math. 23, Springer, Berlin, 1994.

[26] Y. SAAD AND M. H. SCHULTZ, *GMRES: A generalized minimal residual algorithm for solving nonsymmetric linear systems*, SIAM J. Sci. Statist. Comput., 7 (1986), pp. 856–869.

[27] T. P. SAPSIS AND P. F. J. LERMUSIAUX, *Dynamically orthogonal field equations for continuous stochastic dynamical systems*, Phys. D, 238 (2009), pp. 2347–2360.

[28] M. SCHÄFER, S. TUREK, F. DURST, E. KRAUSE, AND R. RANNACHER, *Benchmark computations of laminar flow around a cylinder*, in Flow Simulation with High-Performance Computers II, Notes Numer. Fluid Mech. 48, Springer, Berlin, 1996, pp. 547–566.

[29] M. SCHICK, *Parareal time-stepping for limit-cycle computation of the incompressible Navier-Stokes equations with uncertain periodic dynamics*, Multiple Shooting and Time Domain Decomposition Methods, Contributions in Mathematical and Computational Sciences, Springer International Publishing, 9 (2015).

[30] R. TEMAM, *Navier-Stokes Equations: Theory and Numerical Analysis*, AMS Chelsea, Providence, RI, 2001.

[31] S. TUREK, *Efficient Solvers for Incompressible Flow Problems: An Algorithmic and Computational Approach*, Lect. Notes Comput. Sci. Eng. 6, Springer, Berlin, 1999.

[32] X. WAN AND G. E. KARNIADAKIS, *Multi-element generalized polynomial chaos for arbitrary probability measures*, SIAM J. Sci. Comput., 28 (2006), pp. 901–928.

[33] N. WIENER, *The homogeneous chaos*, Amer. J. Math., 60 (1938), pp. 897–936.

[34] D. XIU AND G. E. KARNIADAKIS, *The Wiener–Askey Polynomial Chaos for Stochastic Differential Equations*, SIAM Journal on Scientific Computing, 24:2 (2002), pp. 619–644.

[35] E. ZEIDLER, *Applied Functional Analysis: Applications to Mathematical Physics*, Appl. Math. Sci. 108, Springer, New York, 1999.